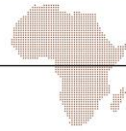


# Spatial Propagation of COVID-19 in the Democratic Republic of Congo

|     |  |
|-----|--|
| 著者  | Otchia Christian Samen   |
| 権利  | Copyrights 日本貿易振興機構（ジェトロ）アジア経済研究所 / Institute of Developing Economies, Japan External Trade Organization (IDE-JETRO) <a href="http://www.ide.go.jp">http://www.ide.go.jp</a> |
| 雑誌名 | アフリカレポート   |
| 巻   | 59   |
| ページ | 49-64  |
| 発行年 | 2021-04  |
| 出版者 | 日本貿易振興機構アジア経済研究所   |
| URL | <a href="http://hdl.handle.net/2344/00052107">http://hdl.handle.net/2344/00052107</a>  |



# Spatial Propagation of COVID-19 in the Democratic Republic of Congo

コンゴ民主共和国における新型コロナウイルスの空間的拡散

Otchia Christian Samen

#### Abstract (要約) :

We combine spatial econometrics with district-level data to assess the spatial spread of COVID-19 in the Democratic Republic of Congo. We find that Kinshasa was the initial hot spot for the outbreak, subsequently spreading to its neighboring districts. Other hot spots emerged in large districts at the borders, such as the Haut-Katanga and Sud-Kivu. Our findings show that districts with a high prevalence of Ebola, Cholera, and other endemic diseases are predicted to have more confirmed cases of COVID-19. We find strong evidence that districts with a high prevalence of conflicts are more susceptible to COVID-19. Our findings also show that meteorological factors such as temperature, physical elevation, and wind speed have played an important role in containing the spread. Taken together, our findings suggest that DRC could have better survived the spread of COVID-19 if it had used the experiences accumulated in the struggle against previous pandemics.

本論文では、地区レベルのデータを利用して空間計量経済分析を行い、コンゴ民主共和国における新型コロナウイルスの感染拡大の状況を検討した。その結果、キンシャサから始まった感染拡大が近隣の地区に波及したこと、また、上カタンガ州や南キヴ州といった国境に接する州も感染拡大の中心地であったことが明らかになった。さらに、エボラ出血熱やコレラ、その他の感染症の感染者が多い地区や、紛争が多発する地区では新型コロナウイルスの感染者が多いことが分かった。気温、標高、風速などの気候条件も感染と関連していた。これらの結果から、過去の感染爆発の経験を活かすことができているならば、コンゴ民主共和国は新型コロナウイルスの流行を現状よりも抑えることができたと思われる。(訳：福西隆弘)

Keywords : COVID-19 Ebola Cholera Conflict Spatial econometrics

## 1. Introduction

The global confirmed cases of COVID-19 have passed 54 million and continues to grow rapidly<sup>1</sup>. In Africa, the incidence of confirmed cases and deaths remains lower than in the rest of the world. As of October 1, 2020, 32 African countries have still not reached 10,000 cases, and the total amount of deaths in the continent remained at less than 50,000. Africa has also done well with daily recoveries, which averaged 79% against 65% in the United States. However, it is worth noting that the cases are rising rapidly with large variations across and within countries. There are many reasons for these new waves, but two stand out. On the one hand, economic needs and political pressure have led governments to loosen movement restrictions across and within borders. On the other hand, people are getting lax on precautions after spending more than nine months under the pandemic. While considerable attention has been paid to the impacts of COVID-19, socioeconomic factors influencing the spatial spread of COVID-19 are much less well understood. It is now a fact that only by addressing the spread of the virus will we tackle the economic and political problems.

We examine the relationship between socioeconomic factors, spatial effects, and the spread of COVID-19 using the Democratic Republic of Congo (DRC) as a case study. This is an important case for several reasons. Most importantly, COVID-19 hit the DRC when the country was already overburdened by Cholera, measles, Ebola, and other endemic diseases such as malaria. Ongoing civil conflicts and security issues also hit the country. An important fear is a mass displacement of the population fleeing conflicts, which may hinder efforts to contain the spread of those diseases. The pandemic and civil war both have a definite impact on communities' productivity, exposing them to food insecurity and malnutrition challenges. Finally, the reliance of the DRC on commodity exports may reduce its capability to respond to the crisis. Macroeconomic responses have led to high inflation, further putting pressure on households and firms (INS 2020). Despite this background, there has been surprisingly little empirical guidance on how the DRC can survive with these threads.

We address three specific questions. First, does the presence of COVID-19 cases in one district make the prevalence of the COVID-19 cases in neighboring districts more or less likely? Second, do high health risk measures correspond to more COVID-19 confirmed cases? And third, what other variables might be correlated with COVID-19 confirmed counts? To answer these questions, we begin by building a novel dataset that includes district-level<sup>2</sup> information of COVID-19 confirmed cases from April 6, 2020, to October 7, 2020, and conduct an exploratory spatial analysis. We find strong spatial spillovers, which are also increasing over time. Our results indicate three main hot spots located in the neighborhoods of Kinshasa, Haut-Katanga, and Sud Kivu. We then explore the potential of combining spatial dependencies and socioeconomic factors to assess the spatial spread of COVID-19 cases. Our findings confirm the importance of modeling spatial factors in evaluating the transmission of the pandemic. We also find that residents of

---

<sup>1</sup> As of October 1, 2020. Source: Johns Hopkins Coronavirus Resource Center

<sup>2</sup> Specifically, we use second-level administrative boundaries, which include territories and cities.



districts with health risk factors and conflicts are more susceptible to have high COVID-19 infection rates. Sadly, our results point to the fact that the experiences accumulated in the struggle against previous pandemics have not been used to contain the current COVID-19 outbreak. We also find that meteorological factors such as temperature, physical elevation, and wind speed have played an important role in containing the spread.

Our paper is related to fast-growing literature on COVID-19, for which we provide a (very) incomplete summary to emphasize our relative contribution. Our study builds on a growing body of work examining the spatial geographic aspect of COVID-19 (Bailey et al. 2020; Coven and Gupta 2020; Guliyev 2020; Kang et al. 2020; Kuchler, Russel and Stroebel 2020; Mollalo, Vahedi and Rivera 2020). Our paper also contributes to extensive literature on COVID-19. While it is difficult to summarize this literature as the number of papers continues to grow, a recent summary can be found in Brodeur et al. (2020) and van Barneveld et al. (2020).

The remainder of the paper is as follows. Section 2 presents background information on COVID-19 and other diseases in the DRC. Section 3 presents the methodology and data. In section 4, we present the results, and section 5 concludes.

## 2. Background

The DRC is prone to epidemics. Recently, the country has faced an unprecedented health crisis, with several epidemic outbreaks co-occurring. More than 288,000 people contracted measles in 2019, with 5,700 deaths. There are over 2,000 reported cases of Ebola and a high prevalence of malaria, with over 7.6 million reported cases, including 7,652 reported deaths. Besides, as a post-conflict country, the DRC continues to face security problems. Armed conflicts still exist in the eastern part of the country and are increasingly concentrated in North Kivu and Ituri provinces. These conflicts continue with periods of varying intensity. This is a big challenge for the country, given its fragility and the deficiency of medical infrastructure, equipment, and personnel.

The DRC has been widely described as a failed state, unable to meet its citizens' basic needs. In addition to affecting the ability to provide public services, state failure has led to a deeply hybrid form of governance where central state rule has become secondary to localized arrangements (De Herdt and Titeca 2019; Pearson 2011; Seay 2013; Devisch 1998). In many DRC provinces, the non-state provision of public health services has been the cornerstone behind the "survival" of the health sector (Seay 2013). The main actors behind these provisions are faith-based organizations, with support from international NGOs and donors. While the localized arrangement can be efficient when the number of actors is small, the lack of coordination and control of joint action and the conflict of interests pose a severe challenge to the provision of the health system in the DRC. This might explain why the DRC has been unable to eradicate many types of epidemics on its soil.

In the DRC, the first COVID-19 case was confirmed in Kinshasa on March 10, 2020. It was an imported case from abroad. The first case of local transmission was reported on March 17, 2020. As of March 20, 2020,



the country had 23 confirmed cases of COVID-19 in Kinshasa, including one death. Of these cases, 15 were imported from other countries, and eight were local transmissions. As shown in Table 1, the DRC government took timely measures to control the spread of COVID-19. The measures consisted mainly of closing the borders, suspending major shopping centers, bars, churches, and schools. In addition to these two initiatives, government officials at the national and provincial levels have taken measures of isolation and containment. For instance, Kinshasa has been completely locked down from the rest of the provinces. Inside Kinshasa, the area of Gombe (business district) was also locked down. Over time, these measures were gradually replaced to keep hand washing, masks, and social distance. Testing was specifically required for travelers.

Table 1: COVID-19 response timeline in 2020

| Date      | Events  |
|-----------|---|
| March 18  | Bars, restaurants, and non-food businesses closure                  |
| March 18  | Gatherings of more than 20 people banned                            |
| March 19  | External border restrictions (High risk countries)                  |
| March 29  | National state of health emergency declared                         |
| April 6   | Curfew (Gombe)  |
| April 17  | Schools and universities closure                                    |
| April 22  | Curfew (Gombe) ends   |
| May 20    | Curfew (Kinshasa)   |
| June 10   | Demission de Mukwege  |
| July 22   | Shops, banks, restaurants, bars, and public transport were reopened |
| August 3  | Schools and universities reopening                                  |
| August 15 | DRC closes bars, restaurants, and non-food businesses reopen        |
| August 15 | External border restrictions were lifted                            |

Source: Author's construction

Lockdown measures were not observed unequivocally, as many households depend on daily work from the informal sectors. Also, several (non-authorized) demonstrations were organized in Kinshasa in July to protest the appointment of the head of the Electoral Commission. Public servants involved in the COVID-19 taskforce also went on strike to demand their unpaid wages and protest their hard working conditions. Perhaps the most significant event was the resignation of the 2018 Nobel peace laureate Doctor Denis Mukwege from the COVID-19 taskforce in Sud Kivu and Ituri. Doctor Mukwege pointed out the lack of testing equipment, a slackening of preventive measures, the impossibility of enforcing barrier measures, and the porosity of borders with the massive return of thousands of Congolese from neighboring countries without having been quarantined.

In addition to measures to control the spread of COVID-19, the government took additional steps to support the economy. In particular, the government designed a multisectoral emergency program evaluated at US\$ 2.3



billion (DRC 2020). The plan was based on three pillars: (i) response to Covid-19, surveillance and strengthening of the health system, (ii) support for macroeconomic stability and recovery, and (iii) risk mitigation and support to the population. Additional support measures directly to households through the provision of free water and electricity services were also executed. Furthermore, the central bank of the DRC created a special refinancing window to support sectors affected by the pandemic. However, all these measures, combined with the growing uncertainties resulting from the exponential increase in contagion, have not mitigated the macroeconomic impact of COVID-19, particularly on growth, inflation, and unemployment (INS 2020).

### 3. Methodology and Data

#### (1) Methodology

Given our interest in the extent to which the presence of COVID-19 cases in one district makes the prevalence of the COVID-19 cases in neighboring districts more or less likely, a natural empirical approach is to examine the spatial autocorrelation. We thus begin by calculating the global Moran's  $I$  index for global spatial correlation (Anselin 1995) as follows:

$$I = \frac{\mathbf{z}^T \mathbf{W} \mathbf{z}}{\mathbf{z}^T \mathbf{z}} \quad (1)$$

$$z(I) = \frac{I - E(I)}{\sqrt{Var(I)}} \quad (2)$$

where  $\mathbf{z}$  is an  $N$ -vector of standardized COVID-19 confirmed cases in the districts,  $\mathbf{W}$  is an  $N \times N$  row-standardized spatial weight matrix (SWM),  $N$  is the number of districts,  $z(I)$  is the standardization of Moran's  $I$ , with  $E(I)$  the expected value of  $I$  and  $Var(I)$  the variance of  $I$  under the spatial randomization.  $E(I)$  and  $Var(I)$  are computed as:

$$E(I) = \frac{-1}{N - 1} \quad (3)$$

$$Var(I) = E(I^2) - E(I)^2 \quad (4)$$

The global Moran's  $I$  is within a range of -1 to 1. A negative value indicates a negative spatial correlation, meaning that districts neighboring a region with high COVID-19 cases show low confirmed cases. A positive value is a sign of a positive correlation in the data. This implies that provinces neighboring a region with high COVID-19 confirmed cases also show high COVID-19 confirmed cases. A value of 0 means that COVID-19 cases are randomly distributed in space as there is no spatial correlation. Finally, the larger the absolute value is, the stronger the spatial correlation.

In a second step, we estimate a spatial autoregressive (SAR) model to explain the spatial spread of COVID-19 confirmed cases using cross-sectional data. In particular, we model the recent confirmed cases for district



$j$  in October 2020,  $(C_{j,t})$ , as a function of lagged cases (July 2020 ( $C_{j,t-3}$ ) or May 2020 ( $C_{j,t-5}$ )) and other predetermined independent variables. We also make use of both a spatial lag of the dependent variable, specified by the spatial contiguity matrix  $\mathbf{W}$ , as well as a spatially lagged error term utilizing the same spatial matrix  $\mathbf{W}$ . The spatial weight matrix is derived using rook contiguity. As such, districts are considered first-order neighbors if they share a common border of non-zero length. For other explanatory variables, the empirical literature on COVID-19, from which the potential explanatory variables could be selected, is too vast and new to review. The rationale for choosing variables is motivated by our research objectives and the brief discussion in the background. In what follows, we consider a broad range of regressors grouped into four categories: meteorological, health risk factors, conflicts, and other socioeconomic factors. We discuss the variables in the next section.

## (2) Data

We have assembled district data on COVID-19 and related variables from several sources. In the DRC, the Multisectoral COVID-19 Response Committee under the Health Ministry maintains a daily database of COVID-19 containing information on the number of infections, death, and recovery. For this study, we use COVID-19 confirmed cases data aggregated bi-weekly from April 6, 2020, to October 7, 2020. In particular, we focus on the number of confirmed infected cases, as the death cases are very small for econometric analysis. Table 2 shows descriptive statistics. While the first COVID-19 case was confirmed in the DRC on March 10, 2020, the number of confirmed cases increased to 168 by April 6. On June 6, the number of reported cases accumulated to 6323 and crossed 8107 on September 19.

Table 2: Confirmed COVID-19 cases (N=190)

| Variable    | Min | p25 | p50 | p75 | p99 | Mean | max  | Date   |
|-------------|-----|-----|-----|-----|-----|------|------|--------|
| $C_{j,t}$   | 0   | 1   | 6   | 157 | 983 | 169  | 8188 | 7-Oct  |
| $C_{j,t-1}$ | 0   | 1   | 6   | 149 | 899 | 157  | 8107 | 19-Sep |
| $C_{j,t-2}$ | 0   | 0   | 5   | 76  | 404 | 116  | 7679 | 4-Aug  |
| $C_{j,t-3}$ | 0   | 0   | 2   | 17  | 325 | 76   | 6323 | 1-Jul  |
| $C_{j,t-4}$ | 0   | 0   | 0   | 2   | 212 | 40   | 3625 | 6-Jun  |
| $C_{j,t-5}$ | 0   | 0   | 0   | 2   | 10  | 4    | 675  | 4-May  |
| $C_{j,t-6}$ | 0   | 0   | 0   | 0   | 5   | 1    | 168  | 6-Apr  |

Source: Author's construction using data from the DRC Multisectoral COVID-19 Response Committee



Table 3: Descriptive statistics (N=190)

| Variable                            | Unit                       | Source      | Observations | Period    | Mean      | Std. Dev. | Min    | Max     |
|-------------------------------------|----------------------------|-------------|--------------|-----------|-----------|-----------|--------|---------|
| GDP (gridded)                       | Digital number values      | aiddata.org | 190          | 2019      | 0.19      | 0.49      | 0.00   | 1.61    |
| Nightlights (mean)                  | Digital number values      | aiddata.org | 190          | 2018      | 0.89      | 1.24      | 0.35   | 5.21    |
| Temperature                         | Degree                     | aiddata.org | 190          | 2017      | 18.63     | 3.19      | 13.08  | 21.50   |
| PM2.5                               | Micrograms per cubic meter | aiddata.org | 190          | 2013      | 17.37     | 3.91      | 9.74   | 30.27   |
| Physical elevation                  | Meters                     | aiddata.org | 190          | 2019      | 683.31    | 312.70    | 205.95 | 1242.73 |
| Wind Speed at 50 meters of altitude | Meters per second          | aiddata.org | 190          | 2019      | 2.28      | 0.45      | 1.58   | 3.26    |
| Hospitalization rate                | %                          | INS         | 190          | 2019      | 1.75      | 1.04      | 0.5    | 4.3     |
| Ebola                               | Cases                      | INS         | 190          | 2019      | 181.54    | 657.34    | 0      | 2921    |
| Cholera                             | Cases                      | INS         | 190          | 2019      | 2635.48   | 4189.46   | 0      | 15050   |
| Tuberculosis                        | Cases                      | INS         | 190          | 2019      | 4725.90   | 2663.06   | 1047   | 21212   |
| Malaria                             | Cases                      | INS         | 190          | 2019      | 461167.30 | 271224.10 | 65259  | 1323229 |
| Meningitis                          | Cases                      | INS         | 190          | 2019      | 430.09    | 362.14    | 61     | 1705    |
| Plague                              | Cases                      | INS         | 190          | 2019      | 0.85      | 3.83      | 0      | 18      |
| Acute Flaccid Paralysis (AFP)       | Cases                      | INS         | 190          | 2019      | 84.03     | 131.79    | 16     | 791     |
| Monkeypox                           | Cases                      | INS         | 190          | 2019      | 96.64     | 192.78    | 0      | 786     |
| Battles                             | Cases                      | ACLED       | 190          | 2019-2020 | 32.94     | 82.91     | 0      | 349     |
| Protests                            | Cases                      | ACLED       | 190          | 2019-2020 | 11.54     | 18.82     | 0      | 68      |
| Riots                               | Cases                      | ACLED       | 190          | 2019-2020 | 8.89      | 14.78     | 0      | 54      |
| Violence against civilians          | Cases                      | ACLED       | 190          | 2019-2020 | 6.68      | 13.53     | 0      | 49      |
| Wageworker                          | Cases                      | INS         | 190          | 2019      | 11.54     | 7.17      | 2.6    | 35.7    |
| Moonlighting                        | Cases                      | INS         | 190          | 2019      | 8.75      | 4.04      | 0      | 24.2    |
| Provincial parks                    | Count                      | INS         | 190          | 2019      | 63.84     | 52.71     | 6      | 190     |
| Population (50 and older)           | %                          | INS         | 190          | 2019      | 4.85      | 1.01      | 2.40   | 6.55    |
| National roads                      | Km                         | INS         | 190          | 2019      | 869.84    | 294.73    | 252    | 1370    |

Note: This table presents descriptive statistics based on 190 districts. The original shapefiles of the DRC contain 240 districts and territories with 190 unique entities and 50 duplicates. The duplicates are entities that are both cities and districts at the same time. Examples include Matadi, Kananga, Goma, among others.





We first use the districts' and territories' administrative boundaries from the Humanitarian Data Exchange (HDX). The data includes the shapefiles of 240 cities and territories, but 50 shapefiles are duplicates of cities. For this study, we remove the 50 duplicates and use 190 unique districts and territories. The regressors are measured in various years, but all are predetermined and dated before March 2020. The National Institute of Statistics (INS) of DRC combines several data to produce non-frequent yearbook statistics. The yearbook also includes information on demographics and other characteristics such as national roads, moonlighters, wageworkers, and hospitalization rates<sup>3</sup>. We obtained data on nightlight intensity<sup>4</sup>, gridded GDP<sup>5</sup>, and meteorological data from aiddata.org. We particularly include temperature, PM2.5<sup>6</sup>, physical elevation<sup>7</sup>, and wind speed<sup>8</sup>. We use conflict data from the Armed Conflict Location & Event Data (ACLED) Project. Table 3 provides variable names, together with their descriptions and descriptive statistics. In the empirical analysis, all the variables are transformed using the inverse hyperbolic sine function to deal with many zero-valued observations.

## 4. Result

### (1) Case distribution

Figure 1 panel A illustrates the district level geographical distribution of the cumulated confirmed Cases of COVID-19 on October 7, 2020. The distribution of confirmed cases is markedly concentrated in the regions near the borders and surrounded by districts with higher than average levels of confirmed cases of COVID-19. Most of the regions in the center have zero or a very small number of infected cases. Kinshasa, the capital city, is a definite outlier as it represents about 75% of COVID-19 counts. Kinshasa has the status of city and province. For better comparison, we present the aggregated COVID-19 case counts at the province level in the panel B of Figure 1. The results reveal that Kongo-Central, Haut-Katanga, and Sud-Kivu have a high concentration of confirmed cases. Since the beginning of the COVID-19 spread, Kinshasa has been a hot spot and influenced the spread of COVID-19 in Kongo-Central first. However, a few regions in the Sud Kivu also revealed high cases in early April. A few districts of Lualaba, Ituri, and Nord-Kivu, become hot spots in July, and we see the progress of clusters of high confirmed cases among neighboring districts. Regarding regions at the center, Figure 1 reveals that they are less hit by COVID-19, mainly due to their remoteness. We see regions such as Kwilu and Kasai have high cases because of their proximity and economic relation with Kinshasa. This indicates that the clustering of lower contamination of COVID-19 among neighboring districts is not random. In the next section, we identify the drivers behind.

<sup>3</sup> Hospitalization rates measure the 25-54-year-old hospitalization for curative diseases.

<sup>4</sup> Nightlight intensity data go from 0 to 63, with higher values implying more intense nightlights.

<sup>5</sup> The GDP data is created from nighttime lights and LandScan population grid to map both formal and informal economic activities.

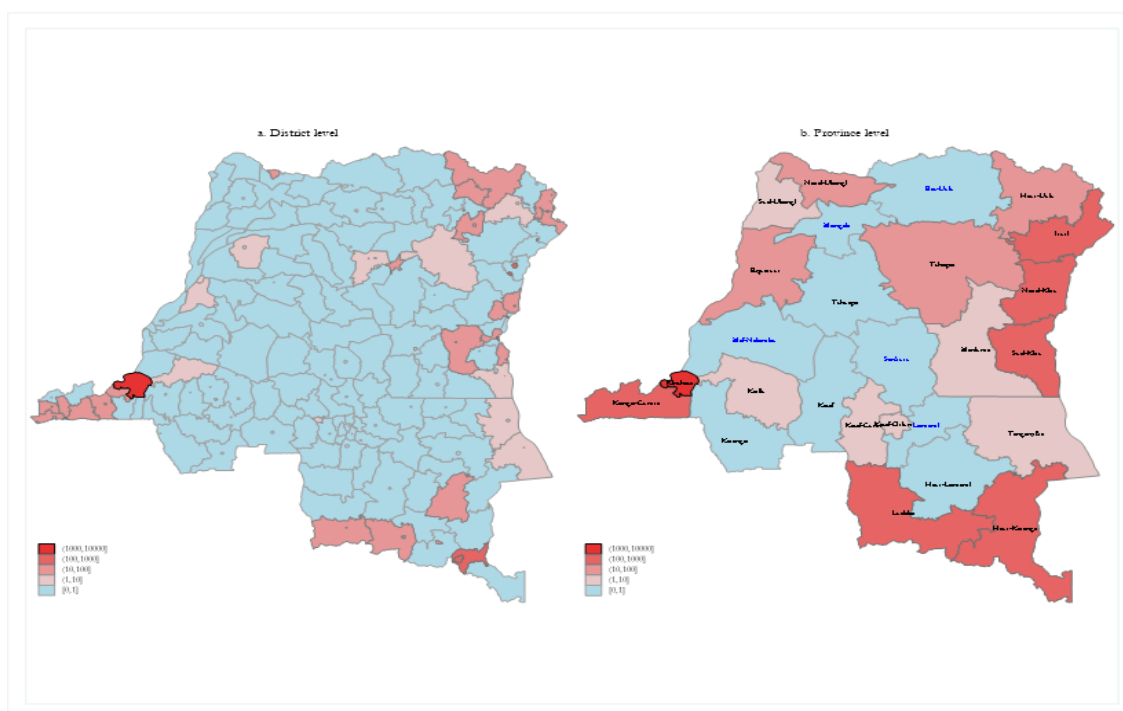
<sup>6</sup> Also known as Particular Matter, PM2.5 describes fine inhalable particles, with diameters 2.5 micrometers and smaller.

<sup>7</sup> Global elevation (in meters) of districts at the height above sea level.

<sup>8</sup> Wind speed potential at 50m height.



Figure 1: Confirmed cases of COVID-19 in the DRC (as of October 7, 2020)



Source: Author's computation using data from the DRC Multisectoral COVID-19 Response Committee

Because districts had their first cases at different times, we normalized each district's case by isolating when each district had its first case to establish a baseline and calculate the average growth rate. Table 4, which presents aggregated results at province level for easy exposure, shows a broad spread across the DRC, with a particularly high concentration of confirmed cases in the West, South-East, and East. The findings show that high-confirmed cases can be seen in Kinshasa and other provinces located at the frontier with a high connection with neighboring countries. Lower confirmed cases are predominately in the center of the country. It should be noted that by the end of September, five districts had no confirmed cases.

Another important finding is that districts with high cases have neighbors with similar characteristics, suggesting a positive spatial autocorrelation in district cases of COVID-19. This is confirmed by the months' variations when each district had its first case (Table 4). Kongo-Central had its first case one month after Kinshasa. Provinces with lower confirmed cases like the Kasai, Kasai-Central, and Kasai Oriental, had their first cases in August or September. A sharp increase was observed in Kasai-Oriental and Nord-Ubangi, mainly because of late contamination. The compound monthly growth rate shows that the number of cases increased by 200% in Kasai-Oriental and 474.46% in Nord-Ubangi. The second group of provinces observed high growth rates (more than 100%) despite discovering the first cases earlier in May. This includes Tshopo, Kongo-Central, Nord-Kivu, Ituri, Sud-Kivu, and Haut-Katanga. Other provinces such as Equateur, Haut-Uele, Kasai-Oriental, Kinshasa, and Lualaba have realized growth rates between 50% and 100%. The last group realized lower rates despite starting earlier. This group includes Kwilu, Sud-Ubangi, Kwango, and Haut-Lomami.



Table 4: Distribution of cases

| Provinces      | Initial cases | confirmed cases | Population adjusted number of confirmed cases in October | Compound growth rate | Months since the first case to October |
|----------------|---------------|-----------------|--|----------------------|--|
| Bas-Uele       |               | 0.00            | 0.00   | 0.00                 | 0                                      |
| Equateur       |               | 0.61            | 9.22   | 96.80                | 5                                      |
| Haut-Katanga   |               | 2.52            | 84.32  | 101.72               | 6                                      |
| Haut-Lomami    |               | 0.39            | 0.39   | 0.00                 | 5                                      |
| Haut-Uele      |               | 5.73            | 44.77  | 98.47                | 4                                      |
| Ituri          |               | 0.47            | 37.02  | 106.92               | 7                                      |
| Kasai          |               | 0.31            | 0.31   | 0.00                 | 3                                      |
| Kasai-Central  |               | 0.34            | 1.01   | 73.21                | 3                                      |
| Kasai-Oriental |               | 0.18            | 0.55   | 200.00               | 2                                      |
| Kinshasa       |               | 13.29           | 647.71   | 91.12                | 7                                      |
| Kongo-Central  |               | 1.08            | 92.91  | 143.91               | 6                                      |
| Kwango         |               | 0.50            | 0.50   | 0.00                 | 5                                      |
| Kwilu          |               | 0.27            | 1.65   | 34.80                | 7                                      |
| Lomami         |               | 0.00            | 0.00   | 0.00                 | 0                                      |
| Lualaba        |               | 13.12           | 71.54  | 76.03                | 4                                      |
| Mai-Ndombe     |               | 0.00            | 0.00   | 0.00                 | 0                                      |
| Maniema        |               | 0.86            | 0.86   | 0.00                 | 2                                      |
| Mongala        |               | 0.00            | 0.00   | 0.00                 | 0                                      |
| Nord-Kivu      |               | 0.56            | 109.40   | 141.14               | 7                                      |
| Nord-Ubangi    |               | 0.96            | 31.82  | 474.46               | 3                                      |
| Sankuru        |               | 0.00            | 0.00   | 0.00                 | 0                                      |
| Sud-Kivu       |               | 0.69            | 53.19  | 106.15               | 7                                      |
| Sud-Ubangi     |               | 1.09            | 2.19   | 25.99                | 4                                      |
| Tanganyika     |               | 2.42            | 2.42   | 0.00                 | 2                                      |
| Tshopo         |               | 0.38            | 19.12  | 165.91               | 5                                      |
| Tshuapa        |               | 0.76            | 0.76   | 0.00                 | 2                                      |

Note: This table presents the distribution of COVID-19 confirmed cases from the 190 districts grouped into 26 provinces. The population-adjusted number of confirmed cases is obtained by dividing the confirmed cases by the district population and multiplied it by one million. The compound growth rate is calculated as the monthly rate of change between the first month where the first cases were reported and the final month of our sample (October).



## (2) Spatial statistics

In the present study, we use the global Moran's  $I$  to investigate the spatial distribution pattern of each district's COVID-19 incidence rate. In the analysis, we use the population-adjusted number of confirmed cases obtained by dividing the confirmed cases by the district population and multiplied it by one million to get the population-adjusted number of confirmed cases. The findings reveal positive spatial autocorrelation patterns for confirmed cases of COVID-19 in the DRC (Table 5). Put differently, the global Moran's  $I$  index indicates highly clustered patterns for the entire period, implying that the distribution of COVID-19 confirmed cases is not random. We also find some interesting temporal changes in global patterns of spatial autocorrelation that are worth noting. In April and May, the Moran's  $I$  index was small and was even smaller in May. However, we see a robust trend of Moran's  $I$  index from June to October, resulting in increased spatial dependence among neighboring districts. The spatial correlations are particularly high in September and October, as the Moran's  $I$  index values are greater than 0.3 (Cressie 1992). It is important to note here that the increasing clustering of COVID-19 cases in June to October appears to be the outcome of a dynamic wave of contaminations induced by protests and demonstrations resulting in expanding clusters of confirmed cases and overall growth in the number of testing.

Table 5: Moran's  $I$  index of spatial autocorrelation

| Date   | Moran's Index | Expected Index | Variance | z-score | p-value |
|--------|---------------|----------------|----------|---------|---------|
| 6-Apr  | 0.03326       | -0.00529       | 0.0200   | 1.9271  | 0.0540  |
| 4-May  | 0.02776       | -0.00529       | 0.0137   | 2.4128  | 0.0158  |
| 6-Jun  | 0.27359       | -0.00529       | 0.0383   | 7.2833  | 0.0000  |
| 1-Jul  | 0.25529       | -0.00529       | 0.0394   | 6.6224  | 0.0000  |
| 4-Aug  | 0.29432       | -0.00529       | 0.0438   | 6.8432  | 0.0000  |
| 19-Sep | 0.37021       | -0.00529       | 0.0491   | 7.6517  | 0.0000  |
| 7-Oct  | 0.40402       | -0.00529       | 0.0510   | 8.0310  | 0.0000  |

Note: This table reports Moran's  $I$  tests for spatial autocorrelation for the COVID-19 confirmed cases for the 190 districts under the null hypothesis of spatial randomization (no spatial autocorrelation). Moran's  $I$  index, z-score, expected index of the Moran's  $I$  and the variance have been calculated using equations 1-4 in the main text.

## (3) Spatial regression

Since we found strong spatial correlations in the previous analysis, we present in Table 6 through Table 9 the estimates from the SAR model. We assume that the confirmed cases count in district  $j$  is affected by confirmed case counts in the previous months and the confirmed cases in district  $j$ 's neighbors. Table 6 presents the results regarding the initial level of development and meteorological factors. Column 1 presents our primary specification, where we include two autoregressive terms,  $C_{j,t-5}$ , and  $C_{j,t-3}$ . The first term corresponds to May, where the lockdown policies were put in place, and the second term is July when these measures started to be gradually removed. The coefficient associated with the autoregressive term of July ( $C_{j,t-3}$ ) is positive and statistically significant. The magnitude is 1.766 and larger than unity. This means that



the COVID-19 pandemic has progressed exponentially after the government removed the preventive health measures. The magnitude is somehow smaller than expected because the reopening of activities was officially announced at the end of July. The coefficient related to May ( $C_{j,t-5}$ ) is negative and estimated at -4.412, implying that lockdown measures had reduced the spread of COVID-19 more than proportionally. Column 2 shows that districts with higher mean GDP are likely to have more confirmed cases. Column 3 introduces nightlights as a proxy of agglomeration and industrialization<sup>9</sup>. We find the magnitude of nightlights is also large, positive, and statistically significant. This implies that districts with larger agglomeration are more likely to have significantly larger confirmed cases. Columns 4 through 7 present the results for the meteorological variables. The coefficient of temperature in column 4 is statistically significant but negative. This shows that districts with lower temperatures are more likely to have higher confirmed cases of COVID-19. We find in column 5 that the coefficient of PM2.5, proxy of air pollution, is positive and statistically significant, meaning that residents in districts with higher levels of air pollution are likely to be more exposed to COVID-19. In column 6, our estimates indicate that residents of high-altitude districts are likely to have low COVID-19 cases, whereas those in districts with low wind speed are likely to have more COVID-19 cases (column 7). This finding broadly supports the recent work (Fernández-Raga et al. 2021; Rendana 2020) linking meteorological factors to COVID-19 confirmed cases.

Table 6: Spatial models of COVID-19 Cases: I

| $C_t$              | (1)                  | (2)                    | (3)                  | (4)                   | (5)                  | (6)                  | (7)                   |
|--------------------|----------------------|------------------------|----------------------|-----------------------|----------------------|----------------------|-----------------------|
| $C_{t-3}$          | 1.766***<br>(0.162)  | 1.290***<br>(0.015)    | 1.286***<br>(0.014)  | 1.285***<br>(0.014)   | 1.285***<br>(0.014)  | 1.284***<br>(0.014)  | 1.283***<br>(0.014)   |
| $C_{t-5}$          | -4.412***<br>(1.501) |                        |                      |                       |                      |                      |                       |
| GDP                |                      | 117.731***<br>(31.871) |                      |                       |                      |                      |                       |
| Nightlights        |                      |                        | 94.325***<br>(9.975) |                       |                      |                      |                       |
| Temperature        |                      |                        |                      | -18.138***<br>(1.680) |                      |                      |                       |
| PM2.5              |                      |                        |                      |                       | 18.453***<br>(1.684) |                      |                       |
| Physical elevation |                      |                        |                      |                       |                      | -9.295***<br>(0.837) |                       |
| Wind Speed         |                      |                        |                      |                       |                      |                      | -42.844***<br>(3.486) |
| $C_t$              | 0.070**<br>(0.033)   | 0.067**<br>(0.032)     | 0.076**<br>(0.039)   | 0.081**<br>(0.036)    | 0.081**<br>(0.039)   | 0.044<br>(0.028)     | 0.043<br>(0.028)      |
| $e. C_t$           | 1.708***<br>(0.075)  | 1.741***<br>(0.057)    | 2.202***<br>(0.076)  | 2.239***<br>(0.066)   | 2.236***<br>(0.067)  | 2.244***<br>(0.064)  | 2.432***<br>(0.072)   |
| Observations       | 190                  | 190                    | 190                  | 190                   | 190                  | 190                  | 190                   |
| LogLikelihood      | -1146                | -1144                  | -1127                | -1121                 | -1120                | -1119                | -1120                 |
| Pseudo R2          | 0.927                | 0.919                  | 0.917                | 0.927                 | 0.928                | 0.930                | 0.928                 |
| Model p-value      | 0.000                | 0.000                  | 0.000                | 0.000                 | 0.000                | 0.000                | 0.000                 |
| Spatial p-value    | 0.000                | 0.000                  | 0.000                | 0.000                 | 0.000                | 0.000                | 0.000                 |

Note: The table reports estimates from a cross-sectional SAR regression where the dependent variable is the COVID-19 confirmed cases in October 2020. Each regression includes the autoregressive term of confirmed cases in July and adds an additional independent variable. Robust standard error in parentheses.

\*  $p < 0.1$ , \*\*  $p < 0.05$ , \*\*\*  $p < 0.01$

<sup>9</sup> For a discussion on the relation between nightlights and industrialization in Africa, see Otchia and Asongu (2020).



A large variety of health risk factors has been associated with the spread of COVID-19. In Table 7, we study several diseases that spread in the DRC between 2017 and 2019. We start in column 1 with hospitalization rates for curative diseases used as a proxy for the local health system. We find that the residents of districts with high hospitalization rates are more susceptible to COVID-19. Column 2 of Table 7 includes confirmed cases of Ebola. We find that districts with a higher prevalence of Ebola have significantly higher confirmed cases of COVID-19. Column 3 includes the prevalence of Cholera and shows that districts with a high prevalence of Cholera are likely to be more susceptible to COVID-19. Columns 4 through column 9 include the district's level prevalence of tuberculosis, malaria, meningitis, plague, AFP, and monkeypox, respectively. The magnitude of tuberculosis, malaria, meningitis, AFP, and monkeypox are positive and statistically significant. The coefficient associated with malaria is relatively small, as compared to tuberculosis and Cholera, for example. This finding should be interpreted with caution, as malaria shares some of the highly recognizable symptoms with COVID-19, such as fever, difficulty in breathing, fatigue, and acute onset headaches. According to Chanda-Kapata, Kapata, and Zumla (2020), a malaria case may be misclassified as COVID-19 if symptoms alone are used to define a case during the emergency period and vice versa. The coefficient associated with plague is found to be negative but not statistically significant. Finally, the second panel of Table 7 shows the spatial lag of the dependent variables and the spatial error lag. Both of these statistics are statistically significant and positive in all the models. This indicates that neighboring districts have significant, positive effects in the COVID-19 confirmed cases, implying that we cannot ignore neighbors' spatial impacts.

Table 7: Spatial models of COVID-19 Cases: II

| $C_t$                | (1)                  | (2)                  | (3)                  | (4)                 | (5)                 | (6)                  | (7)                 | (8)                  | (9)                  |
|----------------------|----------------------|----------------------|----------------------|---------------------|---------------------|----------------------|---------------------|----------------------|----------------------|
| $C_{t-2}$            | 1.287***<br>(0.016)  | 1.285***<br>(0.009)  | 1.285***<br>(0.014)  | 1.282***<br>(0.014) | 1.283***<br>(0.014) | 1.282***<br>(0.014)  | 1.293***<br>(0.016) | 1.282***<br>(0.014)  | 1.292***<br>(0.014)  |
| Hospitalization rate | 13.945***<br>(3.930) |                      |                      |                     |                     |                      |                     |                      |                      |
| Ebola                |                      | 57.095***<br>(1.785) |                      |                     |                     |                      |                     |                      |                      |
| Cholera              |                      |                      | 10.771***<br>(0.838) |                     |                     |                      |                     |                      |                      |
| Tuberculosis         |                      |                      |                      | 7.342***<br>(0.663) |                     |                      |                     |                      |                      |
| Malaria              |                      |                      |                      |                     | 4.902***<br>(0.442) |                      |                     |                      |                      |
| Meningitis           |                      |                      |                      |                     |                     | 10.172***<br>(0.920) |                     |                      |                      |
| Plague               |                      |                      |                      |                     |                     |                      | -13.681<br>(14.382) |                      |                      |
| AFP                  |                      |                      |                      |                     |                     |                      |                     | 13.912***<br>(1.105) |                      |
| Monkeypox            |                      |                      |                      |                     |                     |                      |                     |                      | 19.094***<br>(1.683) |
| $C_t$                | 0.085***<br>(0.031)  | 0.081**<br>(0.037)   | 0.090**<br>(0.037)   | 0.084**<br>(0.037)  | 0.080**<br>(0.035)  | 0.076**<br>(0.038)   | 0.095***<br>(0.033) | 0.041<br>(0.028)     | 0.072**<br>(0.028)   |
| $e.C_t$              | 1.744***<br>(0.057)  | 3.722***<br>(0.106)  | 2.508***<br>(0.093)  | 2.237***<br>(0.067) | 2.239***<br>(0.066) | 2.245***<br>(0.064)  | 1.605***<br>(0.080) | 2.433***<br>(0.072)  | 2.454***<br>(0.078)  |
| Observations         | 190                  | 190                  | 190                  | 190                 | 190                 | 190                  | 190                 | 190                  | 190                  |
| LogLikelihood        | -1145                | -1056                | -1118                | -1119               | -1119               | -1119                | -1149               | -1118                | -1126                |
| Pseudo R2            | 0.927                | 0.975                | 0.935                | 0.929               | 0.929               | 0.930                | 0.926               | 0.930                | 0.915                |
| Model p-value        | 0.000                | 0.000                | 0.000                | 0.000               | 0.000               | 0.000                | 0.000               | 0.000                | 0.000                |
| Spatial p-value      | 0.000                | 0.000                | 0.000                | 0.000               | 0.000               | 0.000                | 0.000               | 0.000                | 0.000                |

Note: The table reports estimates from a cross-sectional SAR regression where the dependent variable is the COVID-19 confirmed cases in October 2020. Each regression includes the autoregressive term of confirmed cases in July and adds an additional independent variable. Robust standard error in parentheses.

\*  $p < 0.1$ , \*\*  $p < 0.05$ , \*\*\*  $p < 0.01$



We next discuss results from SAR models for the set of explanatory variables related to conflicts. The top part of Table 8 describes the effects of variables related to conflicts, while the bottom panel describes the spatial features. As is evident from Table 8, we see a positive correlation between conflicts and COVID-19 confirmed cases. In Column 1, we show that districts with a high prevalence of battles are likely to have more confirmed cases. Column 2 illustrates the districts with high prevalence of protests also are predicted to have high COVID-19 confirmed cases. Columns 3 and 4 show similar patterns in districts with a high prevalence of riots and violence against civilians. The bottom panel of Table 8 demonstrates the importance of including spatial impacts from neighboring districts in all models.

Table 8: Spatial models of COVID-19 Cases: III

| $C_t$                   | (1)                  | (2)                  | (3)                  | (4)                  |
|-------------------------|----------------------|----------------------|----------------------|----------------------|
| $C_{t-3}$               | 1.273***<br>(0.012)  | 1.271***<br>(0.013)  | 1.273***<br>(0.013)  | 1.269***<br>(0.012)  |
| Battles                 | 36.594***<br>(1.855) |                      |                      |                      |
| Protests                |                      | 30.648***<br>(2.200) |                      |                      |
| Riots                   |                      |                      | 33.147***<br>(2.709) |                      |
| Violence against civils |                      |                      |                      | 35.710***<br>(2.041) |
| $C_t$                   | 0.076**<br>(0.039)   | 0.061*<br>(0.036)    | 0.072*<br>(0.038)    | 0.072*<br>(0.037)    |
| $e. C_t$                | 2.967***<br>(0.087)  | 2.485***<br>(0.091)  | 2.253***<br>(0.063)  | 2.751***<br>(0.083)  |
| Observations            | 190                  | 190                  | 190                  | 190                  |
| LogLikelihood           | -1095                | -1110                | -1112                | -1099                |
| Pseudo R2               | 0.958                | 0.944                | 0.945                | 0.955                |
| Model p-value           | 0.000                | 0.000                | 0.000                | 0.000                |
| Spatial p-value         | 0.000                | 0.000                | 0.000                | 0.000                |

Note: The table reports estimates from a cross-sectional SAR regression where the dependent variable is the COVID-19 confirmed cases in October 2020. Each regression includes the autoregressive term of confirmed cases in July and adds an additional independent variable. Robust standard error in parentheses.

\*  $p < 0.1$ , \*\*  $p < 0.05$ , \*\*\*  $p < 0.01$

Table 9 finally focuses on other socioeconomic variables that have been viewed as important in the literature. We start by including the district level share of wagedworkers in column 1. Our results show that districts with higher shares of wagedworkers are likely to have significantly higher confirmed cases. We also examine the case of districts with a high number of moonlight workers in column 2 and found positive and statistically significant effects. Column 3 includes the number of provincial parks as a proxy of tourism-oriented places. We find that the residents of these districts are likely to be more susceptible to COVID-19. We also find in column 4 that districts with a high share of 50+ people are predicted to have more COVID-19 cases. In results not reported here, we find that the gender composition of the population does not matter. Column 5 adds national roads. As expected, we find that highly connected districts are likely to have significantly higher confirmed cases. The bottom panel of Table 9 shows that the neighboring districts have a positive and significant effect on the confirmed cases of COVID-19.



Table 9: Spatial models of COVID-19 Cases: IV

| $C_t$                     | (1)                  | (2)                  | (3)                  | (4)                  | (5)                 |
|---------------------------|----------------------|----------------------|----------------------|----------------------|---------------------|
| $C_{t-3}$                 | 1.277***<br>(0.013)  | 1.296***<br>(0.014)  | 1.280***<br>(0.013)  | 1.287***<br>(0.014)  | 1.286***<br>(0.014) |
| Wageworker                | 23.323***<br>(1.752) |                      |                      |                      |                     |
| Moonlighting              |                      | 23.335***<br>(2.153) |                      |                      |                     |
| Provincial parks          |                      |                      | 15.090***<br>(1.189) |                      |                     |
| Population (50 and older) |                      |                      |                      | 29.341***<br>(2.379) |                     |
| National roads            |                      |                      |                      |                      | 9.002***<br>(0.818) |
| $C_t$                     | 0.041*<br>(0.027)    | 0.047*<br>(0.028)    | 0.038<br>(0.028)     | 0.054*<br>(0.028)    | 0.049*<br>(0.028)   |
| $e. C_t$                  | 2.441***<br>(0.074)  | 2.239***<br>(0.066)  | 2.441***<br>(0.075)  | 2.459***<br>(0.080)  | 2.244***<br>(0.064) |
| Observations              | 190                  | 190                  | 190                  | 190                  | 190                 |
| LogLikelihood             | -1113                | -1120                | -1117                | -1120                | -1120               |
| Pseudo R2                 | 0.932                | 0.926                | 0.931                | 0.928                | 0.928               |
| Model p-value             | 0.000                | 0.000                | 0.000                | 0.000                | 0.000               |
| Spatial p-value           | 0.000                | 0.000                | 0.000                | 0.000                | 0.000               |

Note: The table reports estimates from a cross-sectional SAR regression where the dependent variable is the COVID-19 confirmed cases in October 2020. Each regression includes the autoregressive term of confirmed cases in July and adds an additional independent variable. Robust standard error in parentheses.

\*  $p < 0.1$ , \*\*  $p < 0.05$ , \*\*\*  $p < 0.01$

## 5. Conclusion

We have presented an empirical assessment of the COVID-19 confirmed cases in the DRC from April to October 2020. Overall, we find that the DRC appears to have few confirmed COVID-19 cases and few deaths but a wide variation across the country. This led to an important question: what are the causes of these subnational variations?

To explain why the subnational variations are so high, we have explored whether the spatial autocorrelation, which leads to spillover from one region to another in the case of COVID-19, is present in the DRC. For this purpose, the richness of our data has allowed us to perform a spatial autocorrelation regression and test a variety of factors that have not been addressed in the literature. It has also enabled us to accurately measure the evolution of the spread and observe the effects of socioeconomic variables separately from other components such as the spatial lag and the error lag.

The analysis reveals that the subnational spread of the COVID-19 confirmed counts is correlated with (i) the high prevalence of several epidemics, which is, in turn, explained by the weak health system and by the lack of a coordinated vision and budget, and by (ii) the prevalence of conflict. Our results further confirm that confirmed cases are also associated with connectivity and population characteristics. Finally, we show that meteorological factors can play an essential role in containing the pandemic. Taken together, this study





suggests that countries can learn from previous epidemics' experience, at least in the short run. This is what the DRC failed to do.

## References

- Anselin, Luc 1995. "Local Indicators of Spatial Association—LISA." *Geographical Analysis* 27 (2):93-115. DOI: <https://doi.org/10.1111/j.1538-4632.1995.tb00338.x>.
- Bailey, Michael, Drew Johnston, Theresa Kuchler, Dominic Russel, Bogdan State and Johannes Stroebel 2020. "The Determinants of Social Connectedness in Europe." in *Social Informatics. SocInfo 2020. Lecture Notes in Computer Science*, vol 12467, edited by S. Aref, Cham: Springer. DOI: [https://doi.org/10.1007/978-3-030-60975-7\\_1](https://doi.org/10.1007/978-3-030-60975-7_1).
- Brodeur, Abel, David M. Gray, Anik Islam and Suraiya Bhuiyan 2020. "A Literature Review of the Economics of Covid-19." IZA Discussion Paper No. 13411.
- Chanda-Kapata, Pascalina, Nathan Kapata and Alimuddin Zumla 2020. "COVID-19 and Malaria: A Symptom Screening Challenge for Malaria Endemic Countries." *International Journal of Infectious Diseases* 94:151-153. DOI: <https://doi.org/10.1016/j.ijid.2020.04.007>.
- Coven, J. and A. Gupta 2020. "Disparities in Mobility Responses to COVID-19." Working paper, Stern School of Business, New York University.
- Cressie, Noel 1992. "Statistics for Spatial Data." *Terra Nova* 4 (5):613-617. DOI: <https://doi.org/10.1111/j.1365-3121.1992.tb00605.x>.
- De Herdt, Tom and Kristof Titeca, eds. 2019. *Negotiating Public Services in the Congo: State, Society and Governance*. London: Zed Books.
- Devisch, R. 1998. "Colonial State Building in the Congo, and Its Dismantling." *The Journal of Legal Pluralism and Unofficial Law* 30 (42):221-244.
- DRC 2020. *Programme multisectoriel d'urgence d'atténuation des effets de la COVID-19 en République démocratique du Congo (PMUAIC-19)*. Kinshasa: Ministère du Plan.
- Fernández-Raga, María, Laura Díaz-Marugán, Marta García Escolano, Carlos Bort and Víctor Fanjul 2021. "SARS-CoV-2 Viability Under Different Meteorological Conditions, Surfaces, Fluids and Transmission Between Animals." *Environmental Research* 192:110293. DOI: <https://doi.org/10.1016/j.envres.2020.110293>.
- Guliyev, Hasraddin 2020. "Determining the Spatial Effects of COVID-19 Using the Spatial Panel Data Model." *Spatial Statistics* 38:100443. DOI: <https://doi.org/10.1016/j.spasta.2020.100443>.
- INS 2020. *Mesure de l'impact du COVID-19 sur les Unités Economiques*. Bulletin Numéro 01 : juillet 2020.
- Kang, Dayun, Hyunho Choi, Jong-Hun Kim and Jungsoon Choi 2020. "Spatial Epidemic Dynamics of the COVID-19 Outbreak in China." *International Journal of Infectious Diseases* 94:96-102. DOI: <https://doi.org/10.1016/j.ijid.2020.03.076>.
- Kuchler, Theresa, Dominic Russel and Johannes Stroebel 2020. "The Geographic Spread of Covid-19 Correlates with Structure of Social Networks as Measured by Facebook." CESifo Working Paper Series 8241, CESifo.
- Mollalo, Abolfazl, Behzad Vahedi and Kiara M. Rivera 2020. "GIS-Based Spatial Modeling of COVID-19 Incidence Rate in the Continental United States." *Science of the Total Environment* 728:138884. DOI: <https://doi.org/10.1016/j.scitotenv.2020.138884>.
- Otchia, C.S. and S. Asongu 2020. "Industrial Growth in Sub-Saharan Africa: Evidence from Machine Learning with Insights from Nightlight Satellite Images." *Journal of Economic Studies*. DOI: <https://doi.org/10.1108/JES-05-2020-0201>.
- Pearson, N. 2011. "Case Study: Democratic Republic of the Congo." DFID, Practical Action Consulting, Save the Children, and CfBT Education Trust (<https://infohub.practicalaction.org/bitstream/handle/11283/366190/4f19819e-5154-49ad-8e90-221c0ae4f5bb.pdf?sequence=1>).
- Rendana, Muhammad 2020. "Impact of the Wind Conditions on COVID-19 Pandemic: A New Insight for Direction of the Spread of the Virus." *Urban Climate* 34:100680. DOI: <https://doi.org/10.1016/j.uclim.2020.100680>.
- Seay, Laura E. 2013. "Effective Responses: Protestants, Catholics and the Provision of Health Care in the Post-War Kivus." *Review of African Political Economy* 40 (135):83-97. DOI: <https://doi.org/10.1080/03056244.2012.761601>.
- van Barneveld, Kristin, Michael Quinlan, Peter Kriesler, Anne Junor, Fran Baum, Anis Chowdhury, PN Junankar, Stephen Clibborn, Frances Flanagan, Chris F. Wright, Sharon Friel, Joseph Halevi and Al Rainnie 2020. "The COVID-19 Pandemic: Lessons on Building More Equal and Sustainable Societies." *The Economic and Labour Relations Review* 31 (2):133-157. DOI: <https://doi.org/10.1177%2F1035304620927107>.

(Otchia Christian Samen / Nagoya University)

